

Centrifuge modelling on seismic behaviour of stone architectural heritages

D.-S. Kim

Department of Civil and Environmental Engineering, KAIST, Daejeon, Republic of Korea

H.-J. Park

Schofield Centre, University of Cambridge, Cambridge, UK

ABSTRACT: Many stone architectural heritages include masonry structures that appear to be vulnerable to horizontal dynamic loads such as earthquakes. However, such structures have stood for thousands of years despite numerous historic earthquakes. This study proposes dynamic centrifuge modelling tests as a way of seismic risk assessment in order to find out how stone architectural heritages with masonry structures endured the seismic load, and whether there is any possibility of future earthquake damage. The seismic behaviour of a three-storey, freestanding stone block structure was modelled and tested within a centrifuge. Models were made at three different scales and dynamic tests were conducted using differing centrifugal acceleration fields so that the behaviours could be transformed to an equivalent full-scale prototype and compared. This modelling of models procedure confirms that the seismic behaviour of stone structures can be predicted using scaled-down models. Dynamic centrifuge tests on one fifteenth scale models of two representative stone architectural heritages in Korea were then conducted. The seismic behaviour of the architectural heritages is then predicted in the event of earthquakes.

1 INTRODUCTION

Korea is the location of a vast array of cultural heritages made of stone. The typical cultural heritage sites in the Gyeongju and Buyeo historic areas were once the capitals of the Silla and Baekje Kingdoms, which governed the Korean Peninsula for nearly a thousand years, and led the development of Korean Buddhism. Stone architecture; including pagodas, gates, walled fortresses, grottos, lanterns and bridges, was well-developed within these cultures. Many stone architectural heritages also include masonry structures, which may appear to be vulnerable to horizontal dynamic loading such as earthquakes but, despite appearances, the historical structures of these areas have kept their forms for over a thousand years despite numerous historical records of earthquakes.

Many studies have been conducted on the dynamic behaviour and seismic vulnerability of stone masonry structures. However, analytical approaches and numerical modelling are difficult to perform and the results are often inconclusive. A full-scale shaking table test yields the best data, but is costly. Because friction governs the behaviour of stone masonry structures, reduced scale centrifuge modelling can be an effective alternative. The stress conditions of a scaled model in a centrifuge

test are known to be the same as in a full-scale prototype. Thus, this equivalent stress condition makes it possible to simulate real seismic behaviour using a reduced scale model. This study proposes a dynamic centrifuge test for structural analysis and seismic risk assessment as a means to evaluate safety during future earthquake events.

In this study, the scaling factors were examined through a 'modelling of models' procedure, which was used to evaluate scaling effects. Models were made at three different scales, representing a three-storey rectangular parallelepiped stone structure. The dynamic response of each block was recorded using accelerometers installed in the middle of each block. Acceleration data was collected at different centrifugal acceleration fields (g-levels). Data from two real earthquakes, at Hachinohe and Ofunato, and a sweeping signal were used as input accelerations in the centrifuge. The tests were conducted at different g-levels so that the recorded behaviour of one scale of model at different g-levels could be transformed to simulate an imaginary full-scale test and compared.

Modelling of models confirmed that the behaviour of miniature stone structures against at seismic load can help predict the behaviour of a prototype of the actual architectural heritages. Dynamic centrifuge tests for one fifteenth scaled models of two

representative stone architectural heritages were conducted and seismic behaviour predicted in the event of earthquakes.

2 DYNAMIC BEHAVIOUR OF A STONE MASONRY STRUCTURE

The seismic behaviour of block-like structures which stand free on their foundations, such as ancient monuments and various artefacts, has been the subject of numerous studies. Since the pioneering study of Housner (1963), various other studies have been conducted on the dynamic behaviour of single block structures with square shapes. Housner provided a basic understanding of the rocking behaviour of a block, as well as the mathematical model, for the first time. Ishiyama (1982) classified the behaviour of single blocks into six categories and established a governing equation for each category, through which he studied natural characteristics and mode conversion standards. Spanos & Koh (1984) studied the steady state behaviour of a rigid body by analysing its response to harmonic motion, and Tso & Wong (1989) approached these modes experimentally.

In the case of two or more block systems, determining the governing equations and mode conversion of the entire system becomes difficult analytically because of diverse behaviour at the boundary between blocks. Psycharis (1990) proposed a governing equation, assuming that only rocking takes place in two slender block structures. Spanos et al. (2001) systematically reviewed various analytical, probabilistic and experimental studies of dynamic behaviour in block structures—including the above-mentioned studies. Makris and Konstantinidis (2003) examined the distinct characteristics of the rocking spectrum for a slender rigid block. In their study, the dynamic behaviour of two rigid block structures caused by ground motion were organised analytically according to patterns and numerically compared.

Today, complex numerical analysis of multi-block systems is possible. Shaking table tests and seismic risk assessments are routinely conducted for significant historic stone monuments. Psycharis et al. (2003) presented a numerical investigation on the seismic response of multi drum classical columns in ancient monuments. Kim and Ryu [18] produced a full-scale model of a stone pagoda in the Sang-Gye-Sa Temple that had been damaged by an earthquake in 1936. Konstantinidis & Makris (2005) presented a numerical investigation on the seismic response of the multidrum classical columns of the Temple of Zeus. D’Ayala et al. (2008) analysed a series of shaking-table tests on three 1/10-scale 3 dimensional dry masonry models.

Peña et al. (2008) described the dynamic behaviour of various free-standing block structures under seismic excitation using 1 g shaking table tests. D’Ayala & Ansal (2012) designed “Risk Assessment of Cultural Heritage Buildings” to address the vulnerability of cultural assets, specifically buildings with global cultural heritage value.

The dynamic behaviour of actual stone architectural heritages during a seismic event involves complex behaviours combined by sliding and rocking motions. In the case of multi-block systems, there are many analytical and numerical difficulties when trying to predict and understand the various modal characteristics of the featured materials and interactions between units. Currently, a full-scale 1 g shaking table test is the most reliable method for acquiring useful data on structural behaviour, but these tests are time and resource intensive.

This study presents a dynamic centrifuge test to be used to evaluate the seismic behaviour of stone structures for use in seismic risk assessments of architectural heritages. For multi-block systems, the characteristics of the friction between stone units have a significant effect on the behaviour of the structure. The centrifuge test described in this paper simulates N times gravity accelerations for a $1/N$ scaled model. When an appropriate scaling law is used and the material used in the model has the same density as the real structure, the seismic behaviour can be observed under the same stress conditions as those found in nature. Therefore, this method is a useful alternative to numerical analysis and full-scale shaking table tests. However, limitations exist within this method, in that it is difficult to reproduce the same surface roughness in modelled stone units and a full-scale prototype.

Scaling laws are a main consideration in testing a full-sized prototype and a small scale model. The laws used in centrifuge testing are listed in Table 1 (Taylor, 1995). In a centrifuge test, the stress conditions are the same as in the full-size prototype in terms of gravity direction and horizontal direction. This equivalent stress condition supports the possibility of accurately simulating

Table 1. Scaling laws for dynamic centrifuge tests.

Quantities	Scaling factors (prototype/model)
Displacement, length	N
Acceleration, gravity	N^{-1}
Mass	N^3
Density	1
Stress	1
Strain	1
Time (dynamic)	N

the seismic behaviour of historic stone monuments in a dynamic centrifuge test on a reduced scale model.

3 MODELLING OF MODELS FOR EVALUATION OF SEISMIC BEHAVIOUR OF STONE MASONRY STRUCTURES

3.1 Experimental setup for modelling of models

The study was conducted at the recently established centrifuge facility at the KOCED Geotechnical Centrifuge Center at KAIST (Kim et al., 2013a, Kim et al., 2013b). The centrifuge is able to simulate seismic motion by spinning at a desired centrifugal acceleration. The KOCED earthquake simulator used in this research is an electro-hydraulic-servo type with a rotation radius of 5.0 m and a maximum capacity of 240 g-ton. This earthquake simulator can reach 40 g of shaking acceleration with no payload and 20 g shaking acceleration for a payload of up to 700 kg. 40 g of centrifuge acceleration is equivalent to a Peak Ground Acceleration (PGA) of 0.5 g. Korean seismic design has a maximum seismic design acceleration (for rock outcrops) of 0.22 g.

The ‘modelling of models’ technique was performed on a three-storey rectangular parallelepiped stone structure. Each storey level consisted of one block—each with identical size, mass and contact surface properties. Models were made at three different scales so that tests could be performed at varying g-levels, the behaviour scaled up to full-scale and then compared in order to simulate the behaviour of one full-scale prototype. The tests were conducted using three sets of differently scaled models in separate test sets. For example, the dynamic motions of models 1, 2, and 3 were recorded at centrifuge accelerations of 10 g, 15 g, and 20 g, respectively. These three test results, all at the same model scale, were then aggregated as prototype 1. This was labelled as test set 1. Table 2 summarizes the entire experimental setup.

The stone used in the experiment was Hwangdeung stone, a type of homogenous granite. All the contact surfaces were cut using a water jet. The density of the stone specimen was 2.67 t/m³ and the shear wave velocity of the specimen was 2037 m/s, obtained using a Free-Free Resonant Column (FFRC) test (Stokoe et al., 1994). Data from two real earthquakes was used as the input: the Ofunato earthquake with high short-period accelerations and the Hachinohe earthquake with high long-period accelerations. In addition, a sweeping signal within the shaking frequency range was used, as shown in Figure 1. The excitation inputs were applied in the transverse and longitudinal directions. Three to four shakings events were conducted in each earthquake simulation, from the lowest acceleration to the PGA with a 2400 year return period level (PGA of 0.07 g to 0.28 g in prototype for each test set).

The stacked blocks of the model were mounted on a compacted soil layer. The acceleration of each block was recorded using PCB353B17 (PCB Piezotronics) accelerometers placed in the middle of each block and the data subsequently analysed. The experimental method for test set 1 and the location of the accelerometers are shown in Figure 2.

Dynamic centrifuge tests were conducted at several g-levels for each model scale. For each set of models, the acceleration values were measured in each block and used to predict the behaviour of an imagined full-scale, three-storey prototype. The parameters used for comparison were the peak acceleration in time domain and predominant frequency in the frequency domain.

3.2 Test results in time domain

The procedure for comparing the experimental results of a model at 1/N scale is as follows. First, the acceleration was recorded at the ground surface, first floor, second floor and third floor, respectively. Second, these measured values were transformed into equivalent full-scale values by applying the scaling laws shown in Table 1. Meaning that time was multiplied by N times, and

Table 2. Experimental setup for the modelling of models.

	Model 1	Model 2	Model 3	Prototype size (W × D × H, m)
Size of one block (W × D × H, cm)	36 × 18 × 9	24 × 12 × 6	18 × 9 × 4.5	
Mass of one block (kg)	15.6	4.61	1.95	
Storey (the number of blocks)	3	3	3	
<i>Centrifugal acceleration (g-level)</i>				
Test set 1 (prototype 1)	10 g	15 g	20 g	3.6 × 1.8 × 0.9
Test set 2 (prototype 2)	20 g	30 g	40 g	7.2 × 3.6 × 1.8
Test set 3 (prototype 3)	30 g	45 g	60 g	10.8 × 5.4 × 2.7

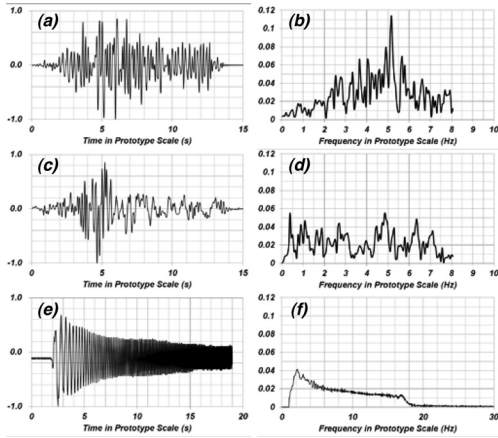


Figure 1. Time histories and frequency contents of input signals for shaking: (a), (b) Ofunato earthquake record; (c), (d) Hachinohe earthquake record; (e), (f) sweeping signal.

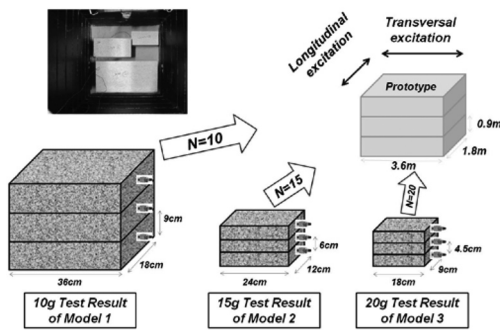


Figure 2. The experimental setup for test set 1.

the acceleration amplitude was multiplied by $1/N$ times from the experimental results of N g state. Third, peak accelerations were determined for comparison. This was done for each model scale so that the experimental results of the three model types could be compared at a full-size prototype scale. Because it is difficult to keep the peak ground surface acceleration constant, the results were normalised by dividing the accelerations recorded at each block by the ground surface acceleration. Finally, comparisons were made between the average values of each model test result.

Following the above procedure, peak acceleration values were recorded at centrifuge accelerations of 10 g, 15 g and 20 g, simulating the Hachinohe earthquake in the transverse direction for the first prototype in as shown in Figure 3. Figure 3(a) shows the acceleration recorded at the each height of the model. Time dependant signals

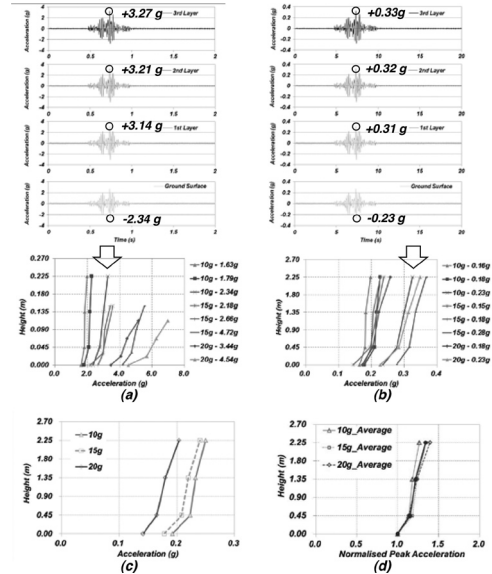


Figure 3. Typical test results of test set 1 for peak acceleration: (a) typical acceleration signal and peak acceleration values in model scale; (b) acceleration values in prototype scale; (c) averaged acceleration values; (d) comparison of normalised averaged acceleration values.

were recorded for each block and the peak acceleration values were obtained. Peak acceleration values were recorded for three excitations at 10 g and four excitations each at 15 g and 20 g. Figure 3(b) shows the accelerations that were applied with the scaling laws for the prototype structure from Figure 3(a). The legend of the peak acceleration diagram in Figures 3(a) and 3(b) represents the centrifugal acceleration level and peak ground acceleration value.

In Figure 3(c), average values at each g-level are shown. Finally, in Figure 3(d), normalised average values are shown. In the case of peak acceleration values, amplification patterns at each height were similar, with a 5.7% maximum error, centred around the average value. The peak acceleration values were significantly different between model 1 (10 g), model 2 (15 g) and model 3 (20 g), as shown in Figure 3(a). However, after applying scaling factors and normalising each peak acceleration value, a consistent amplification pattern can be seen for a given prototype, as shown in Figure 3(d).

Figure 4 shows the comparative graph of averaged peak acceleration values in prototype scale and the amplification patterns for all test sets. The left hand set of figures pertain to transversal excitation (long-length direction, Fig. 2), and the right figures pertain to the longitudinal direction. The maximum errors, centring on average values,

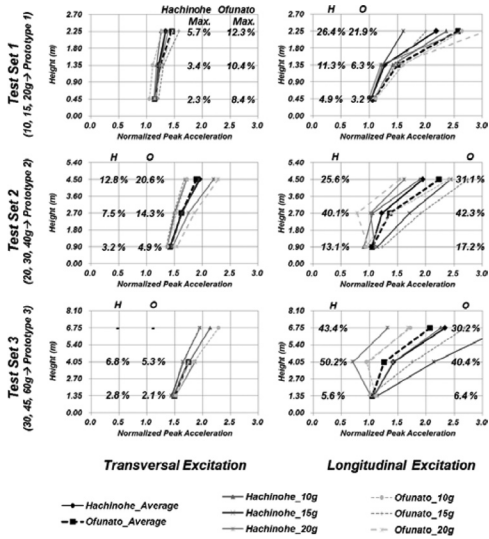


Figure 4. Comparison of averaged peak acceleration values in prototype scale.

are noted for each test set (1, 2 and 3), each input signal (Hachinohe and Ofunato earthquake) and each shaking direction (transversal and longitudinal).

When examined according to the shaking direction, the error values were higher for longitudinal shaking compared to transversal shaking. The error was higher in the short axis of the rectangular models compared to the long axis. In the case of transversal excitation, the amplification pattern was consistent with height. Maximum errors of 12.8% and 20.6% occurred at the third storey for the Hachinohe and Ofunato earthquake simulations, respectively. Conversely, the amplification varied with height for longitudinal excitation. The amplification ratio between the first and second storey differed from that between the second and third storey. For two cases in test set 2 and for two cases in test set 3, the peak accelerations were less in the second storey. This can be explained by the greater complexities of displacement and rocking behaviour in taller, three-storey masonry structures facing the shaking direction.

Overall, the error values for the peak acceleration were highest for test sets 2 and 3. In other words, the error was greater as the centrifuge test increased in g-level. In addition, acceleration data from the third storey block that was not measurable in the 60 g state in test set 3 is not shown graphically. As the g-level increased, the change in the measured results became more pronounced and the error values became greater. In most cases, however, the amplification characteristics of acceleration in the

time domain could be obtained using scaling laws despite experimental errors.

3.3 Test results in frequency domain

The predominant frequency was identified in the frequency domain, in which amplification takes place according to height for each setup. As with the time domain, test sets of the same scale were compared. The acceleration signals at model scale were converted to the frequency domain. They were transformed to full-size prototype scale by applying a scaling law of 1/N times frequency and 1/N times spectral acceleration. Results of shaking using sweeping signals in the frequency domain were compared, these had relatively wide and even frequency contents, as shown in Figure 1(f).

Figure 5 shows the frequency signals for transverse excitation at prototype scale by applying the general scaling law. In the case of transverse excitation, the frequency contents in the full-size prototype scale for the three results of test set 1 were amplified with height, at 12.6 Hz to 14.8 Hz. These were derived from a 131 Hz peak in model 1 (10 g), a 222 Hz peak in model 2 (15 g) and a 253 Hz peak in model 3 (20 g). The predominant frequencies in model scale showed large differences between the three models. However, after applying scaling factors, a consistent predominant frequency range could be obtained for a given prototype.

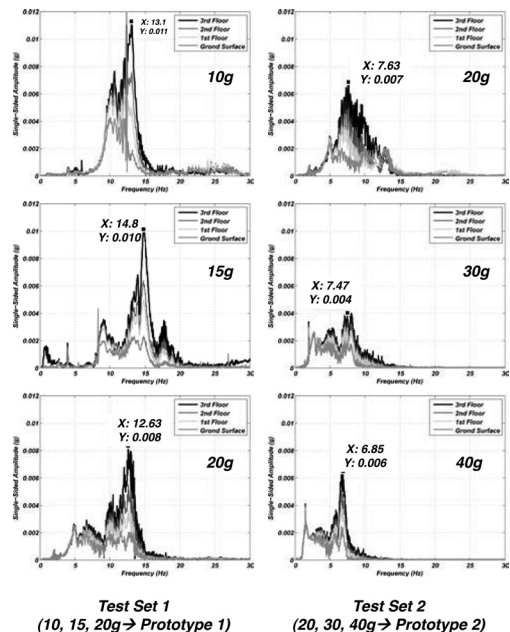


Figure 5. Frequency domain signals obtained from test sets 1 and 2 for transversal excitation in the prototype scale.

The frequency contents at 6.8 Hz to 7.6 Hz were amplified in test set 2 and the frequency contents at 4.5 Hz to 6.8 Hz were amplified in test set 3. For the majority of test results, it was found that acceleration amplification took place and the frequency ranges generally coincided.

To determine if these predominant frequencies could align with the natural frequencies of a real three-storey stone structure, theoretical solutions for rocking and sliding motions of a single block were used for comparison. Those solutions are rocking (Borowicha, 1943, Gorbunov-Possadov & Serebrajanyi, 1961) and sliding (Bycroft, 1956, Barkan, 1962) motion solutions in a soil-foundation system. In this theoretical approach, it was assumed that the stone structure was composed of units with the same shape as a single block and there was no damping effect.

Natural frequency and resonant frequency of rocking vibrations (Fig. 6(a)) of a rigid rectangular foundation in prototype scale are found in Equations (1) and (2) and those for sliding vibrations (Fig. 6(b)) are founded in Equations (3) and (4). Theoretically, natural frequency in the 1/N model become N times of the natural frequency of the prototype when a scaling factor for mass m (1/N³) and length term r₀, D, H and W (1/N) are applied.

The natural frequency of rocking motion of the single block structure of Housner (1963) was as follows in Figure 6(c) and Equation (5). Here, if a scaling law for an acceleration of gravity g and a radius of rotation R is applied, the natural frequency in the 1/N model becomes N times the natural frequency of the prototype like Equation (6). In the case of multi-layered block structures, a scaling law should exist for various dynamic behaviours including rocking, and this should be examined on an experimental basis. Housner's rocking motion assumed that a relatively slender rigid block can oscillate about the centre of rotation, O, when it undergoes rocking as shown in Figure 6(c). Therefore, the theoretical solutions for rocking and sliding motions of a single block in the soil-foundation system can be more adoptable

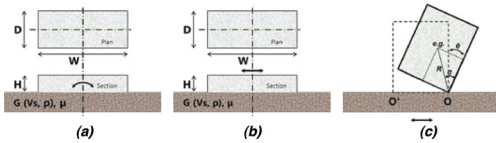


Figure 6. Theoretical approaches for rocking and sliding motion of a single block: (a) rocking motion in the soil-foundation system; (b) sliding motion in the soil-foundation system; (c) Housner's rocking motion of a single block structure.

in order to allow comparison with experimental observation.

$$f_{n, prototype} = \frac{1}{2\pi} \sqrt{\frac{k_{\theta}}{I_0}} = \frac{1}{2\pi} \sqrt{\frac{8Gr_{0,p}^3}{m_p \left(\frac{r_{0,p}^2}{4} + \frac{H_p^2}{3} \right)}} \quad (1)$$

$$f_{n, prototype} = \frac{1}{2\pi} \sqrt{\frac{k_{\theta}}{I_0}} = \frac{1}{2\pi} \sqrt{\frac{G}{1-\mu} \frac{F_{\theta} D_p W_p^2}{m_p \left(\frac{r_{0,p}^2}{4} + \frac{H_p^2}{3} \right)}} \quad (2)$$

$$\text{where } r_{0,p} = \sqrt[4]{\frac{D_p W_p^3}{3\pi}}, F_{\theta} = \begin{cases} 0.6 \text{ at } W/D = 2 \\ 0.44 \text{ at } W/D = 0.5 \end{cases}$$

$$f_{n, prototype} = \frac{1}{2\pi} \sqrt{\frac{k_x}{m_p}} = \frac{1}{2\pi} \sqrt{\frac{32(1-\mu)Gr_{0,p}}{(7-8\mu)m_p}} \quad (3)$$

$$f_{n, prototype} = \frac{1}{2\pi} \sqrt{\frac{k_x}{m_p}} = \frac{1}{2\pi} \sqrt{\frac{2(1+\mu)GF_x \sqrt{D_p W_p}}{m_p}} \quad (4)$$

$$\text{where } r_{0,p} = \sqrt{\frac{D_p W_p}{\pi}}, F_x = \begin{cases} 0.95 \text{ at } W/D = 2 \\ 1.1 \text{ at } W/D = 0.5 \end{cases}$$

$$f_{n, prototype} = \frac{\sqrt{m_p g_p R_p / I_{0,p}}}{4 \cosh^{-1}(1/(1-\theta/\alpha))} = \frac{\sqrt{3g_p / 4R_p}}{4 \cosh^{-1}(1/(1-\theta/\alpha))} \quad (5)$$

$$f_{n, model} = \frac{\sqrt{3g_m / 4R_m}}{4 \cosh^{-1}(1/(1-\theta/\alpha))} = \frac{\sqrt{3(Ng_p) / 4(R_p / N)}}{4 \cosh^{-1}(1/(1-\theta/\alpha))} = N f_{n, prototype} \quad (6)$$

Figure 7 shows a comparison between the observed amplified frequency (i.e. predominant frequency) range in all test sets and the theoretical natural frequencies for rocking and sliding motions of a single block. The upper figures show transversal excitation and the lower figures show longitudinal excitation. The peak frequency and amplification range from the test results and the

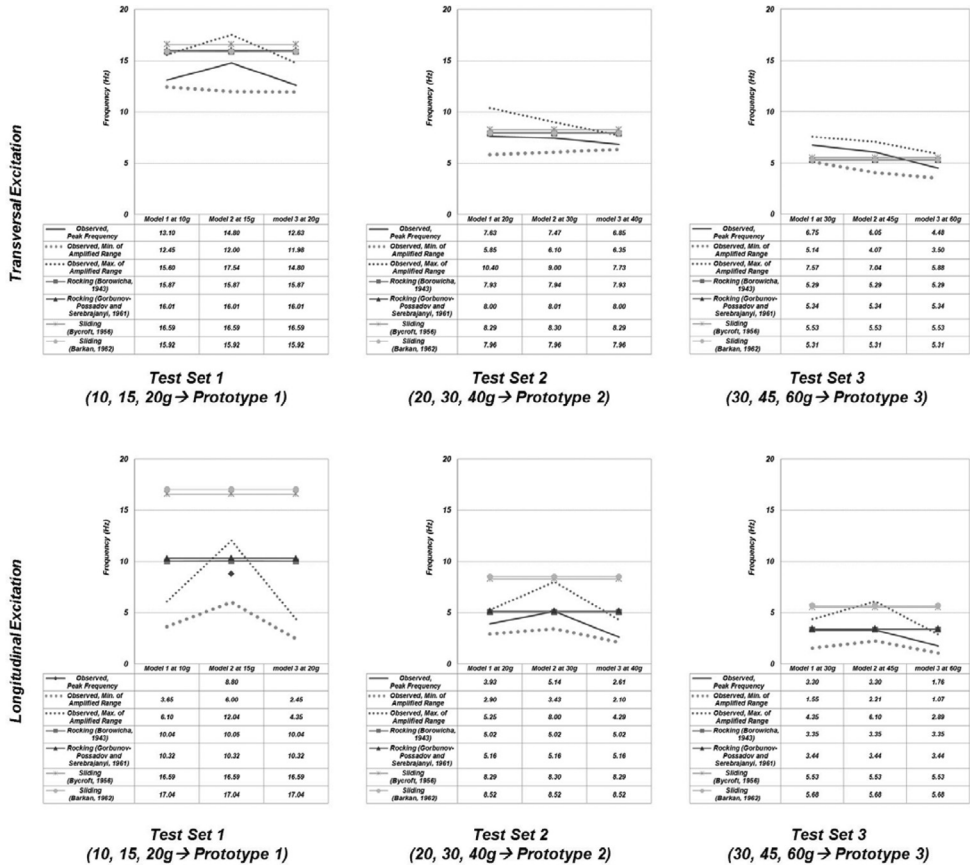


Figure 7. Comparison between observed predominant frequency range and theoretical natural frequency for rocking and sliding motion of a single block in prototype scale.

natural frequency using theoretical equations are also tabulated. It was assumed that the shear wave velocity of the ground, which was considered to be compacted weathered soil, was 200 m/s, mass density was 1800 kg/m³ and Poisson's ratio was 0.33.

In the case of transversal excitation, the natural frequency ranges of rocking and sliding had theoretically similar values. The predominant frequency range of the test results, after application of the scaling factors, was also within a similar range. Conversely, for longitudinal excitation, the natural frequencies of rocking and sliding had different ranges. The predominant frequency range of the test results was closer to the theoretical rocking motion range.

The earthquake simulator used in the tests had an excitation frequency range of 40 Hz to 300 Hz at the model scale. Therefore, when performing the 'modelling of models' procedure, if the same seismic wave was used at each g-level, the scaled frequency would not conform exactly at the full-size

prototype scale. For example, shaking energy exists in the range of 4 to 30 Hz at the 10 g level and in the range of 2 to 15 Hz at the 20 g level. Three models were set up in three test sets because it was difficult to predict the resonant frequency of masonry structures in advance, and the excitation frequency ranges of the earthquake simulator were predetermined.

For determination of the model size (or operating g-level) in a dynamic centrifuge test, the predicted natural frequency range of the target structure, excitation frequency ranges of the earthquake simulator, maximum operational acceleration of the centrifuge, maximum shaking acceleration of the earthquake simulator, mass of the model, and the size of the container must be systematically considered.

Through a comparison of test and theoretical results, it was revealed that the acceleration amplification characteristics and the predominant frequency ranges of the three storey block fell

between theoretical predictions and the observed results. Additionally, this proves that the generalised scaling law can be applied to dynamic behaviour of masonry structures (Park & Kim, 2013).

4 EVALUATION OF THE SEISMIC RESPONSE OF STONE PAGODAS

4.1 Stone architectural heritages and seismic risk assessment

Architectural heritage is an invaluable part of human culture that reflects our people's history. Society has an obligation to preserve this heritage safely in order to pass it on to future descendants. As architectural heritages are always exposed to the outside, they need to be protected against natural disasters and accidents caused by social and environmental changes.

Among numerous architectural heritages of the Silla and Baekje Dynasties, two stone pagodas; the three storied stone pagoda at Bulguksa Temple (UNESCO World Heritage inscribed in 1995, National Treasures No. 21, named the S3 pagoda in this paper) and the five-storied stone pagoda of Jeongnimsa Temple site in Buyeo (National Treasures No. 9, named the J5 pagoda in this paper), are the most representative of the architectural assets. The S3 pagoda demonstrates the representative architectural style of the Silla Dynasty (57 BC–935 AD) and the J5 pagoda represents the architectural history of the Baekje Dynasty (18 BC–660 AD). These pagodas show the remarkable beauty of symmetry and stable proportions between layers or floors. In the case of the S3 pagoda, historical earthquake records exist.

This study attempts to propose dynamic centrifuge tests as a method of seismic risk assessment in order to discover how stone architectural heritages with masonry structures have endured seismic load, and whether there is any possibility of future earthquake damage. In Section 3, the stress conditions and scaling laws for seismic behaviour of stone blocks within a centrifuge were examined and the modelling of models for stone blocks performed. Modelling of models confirmed the possibility that the behaviour of miniature stone structures under seismic load can help predict the behaviour of a prototype of the actual architectural heritages.

In this study, site investigation and ground response analysis for earthquakes have been performed. Then, with the results, 1/15 scale models of two stone pagodas have been produced and dynamic centrifuge tests performed. The variations in peak acceleration with height and frequency contents at each height were measured and

calculated for various dynamic motions in a 15 g centrifugal gravity field. Through these studies, the dynamic behaviour and seismic risk to the prototype of these stone pagodas have been assessed (Park et al., 2013a).

4.2 Two representative pagodas of Korea

This study evaluates the seismic performance of two representative stone pagodas in Korea. The S3 pagoda is also known as Seok-ga-tap (Sakyamuni pagoda) and is one of the finest architectural achievements of the Unified Silla Dynasty, and a structure for which historical earthquake records exist. The construction of the Bulguksa temple began in 742 AD and the S3 pagoda was at risk on two separate occasions due to earthquakes. The pagoda was destroyed and reconstructed in 1024 AD and 1038 AD, respectively. In 1013 AD, an earthquake damaged the S3 pagoda and part of the temple walls; in 1036 AD, an earthquake caused serious damage to the main staircase to the south of Buddha gate, accessory facilities, the lower Buddha gate and multiple servants' quarters. Seok-ga-tap, which was still under repair from previous damage, nearly collapsed. Figures 8(a) and 8(b) show pictures of the S3 pagoda and the Bulguksa Temple taken in 1915 and pictures of the S3 pagoda taken in recent years (NRICH, 2007).

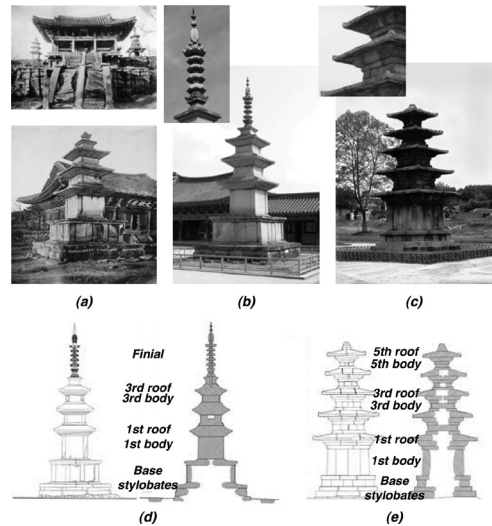


Figure 8. Two representative stone pagodas: (a) pictures of the S3 pagoda and Bulguksa Temple taken in 1915; (b) pictures of the S3 pagoda taken in recent years; (c) pictures of the J5 pagoda; (d) the south elevation and east-to-west cross section of the S3 pagoda; (e) the south elevation and east-to-west cross section of the J5 pagoda (NRICH, 2007, Buyeo-gun & NRICH, 2009).

The S3 pagoda is a stone pagoda with a three-storey body on the two storey base stylobate. The first floor and upper floors have interlacing layers of body and roof stone on each floor. The height of the base stylobate and body is properly balanced, giving a sense of beautiful stability and proportion. The base stylobate or body has no carvings on the surface, which gives it a clean appearance. Beautifully proportioned and elegantly balanced, it is a model pagoda of its time. It is structured with a total of 43 pieces: 20 base stylobate pieces, 6 pagoda body pieces and 17 finial pieces.

The J5 pagoda is considered to be representative of pagodas of the Baekjae Dynasty, as is the S3 pagoda of the Silla Dynasty. It is highly valued as one of the two last remaining stone pagodas from the Baekje Dynasty (Fig. 8(c)). The five-storey body stands on a narrow and low base stylobate and each stylobate is fixed by a pillar stone. Each corner of the pagoda body in each floor holds a pillar stone using the Beheullim technique, where a pillar's upper and lower extremities are narrow while its middle is convex. Thin and wide roof stones cover the edges of the eave displays. The pagoda is valuable in that it has the typical form of a wooden building, e.g. a thin stylobate, with pillars exhibiting the Beheullim technique and thin and wide roof stones. Overall, it is a beautiful piece of art with sophisticated and refined figurative beauty and elegant grace.

On top of the fifth roof stone lies a half-circle stone piece, considered to be the base of a finial and upturned bowl. The body of the first floor is composed of 12 separate pieces. Each corner holds a pillar and each side comprises two slabs of stone. From the second floor, the height of each floor decreases dramatically, giving the pagoda a sense of continuity with the roof stones. The size of the contact area of the bodies becomes smaller moving upwards. The south elevation and east-to-west cross section of the two pagodas are shown in Figures 8(d) and 8(e).

4.3 Site investigation and site-specific ground response analysis

Every architectural structure has its base on the ground, and the stability of the ground is directly related to the stability of the structure (Park et al., 2012). Since ground motion is significantly affected by local site effects, the composition of the entire soil strata, determined by seismic investigations, was utilised in the analyses. Site investigations and ground response analyses were performed to create the earthquake record to be applied to the lower part of the pagoda model in centrifuge tests.

In order to design the seismic coefficient of the architectural heritage site, the level of designed

ground motion was estimated for the site. This study adopted the special structures and seismic class I structures at collapse level of the earthquake, which is equivalent to earthquakes with 2400 year and 1000 year return periods, respectively. The designed rock-outcrop accelerations at Gyeongju and Buyeo were 0.20 g for a 2400 year return period earthquake and 0.14 g for a 1000 year return period earthquake based on the Korean seismic hazard map (Park et al., 2013b).

For the S3 pagoda site, two analyses were performed on the ground: a 1-dimensional ground response analysis using the SHAKE programme (Schnabel et al., 1972) and a 2-dimensional ground response analysis using the FLAC programme (Itasca Consulting Group, 2001) considering irregular surface topography. The result showed that the 2400 year return period earthquake caused 1.45 times amplification in 2-dimensional analysis and 1.65 times amplification under 1-dimensional analysis of rock outcrop peak acceleration. The 1000 year return period earthquake caused 1.74 times amplification under both 1-dimensional and 2-dimensional analyses. The natural frequency of the ground was estimated at 0.13–0.15 seconds (6.7–7.7 Hz).

For J5 Pagoda site, 1-dimensional ground response analysis was performed using the SHAKE programme. The results showed that a 2400 year return period earthquake caused 1.64 times amplification and the 1000 year earthquake caused 1.60 times amplification of acceleration. The natural frequency of the ground was estimated as 0.17–0.18 seconds (5.6–6.0 Hz).

Based on the ground response analyses, the Hachinohe and Ofunato earthquake motions to be applied to the lower part of the two pagoda models in the centrifuge tests were obtained. In the centrifuge test, the earthquake motions were used as input motions after scaling for each maximum acceleration level.

4.4 Centrifuge testing programme

In this study, a 1/15 sized model was produced. The size of the model was determined in consideration of the size of the container used for a dynamic centrifuge test, anticipated bandwidth of the response frequency and feasibility of the model building. In the dynamic centrifuge test, 15 g of centrifugal force was applied vertically, which is 15 times the gravity acceleration, to a 1/15 scaled model in consideration of its stress conditions and scaling laws.

Two pagodas were built with granite as shown in Figures 9(a) and 9(b). Several studies have been conducted to trace the location of origin of the rocks and a scientific evaluation of their deterioration was conducted (Buyeo-gun, 2005, Kim et al., 2005,

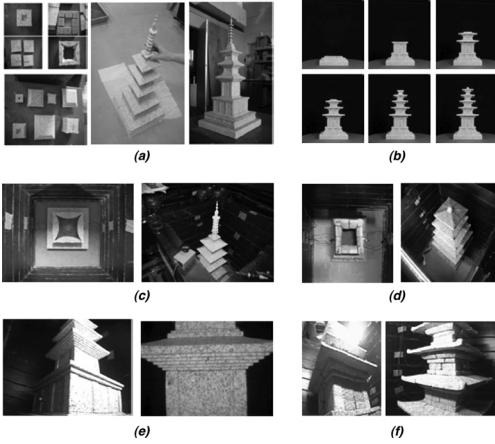


Figure 9. Building process and dynamic centrifuge test procedure for two pagoda models: (a), (b) making each stone for two pagodas; (c), (d) building each stone block; (e), (f) monitoring within the container used in the earthquake simulator.

Lee et al., 2007). Hwang-deung stone was also chosen to build the model to give it similar crack-proof homogeneous properties to the original's stone material. Figure 9 shows the building process of the 1/15 scale model of the two pagodas.

Three types of input signals were used for the shaking events, including the Ofunato and Hachinohe earthquake records and a sine sweeping signal within the shaking frequency range as shown in Figure 1. The width of usable excitation frequency ranges of 30~300 Hz in the models. This means that given the similitude ratio of a 15 g model, the actual pagoda structure will receive signals in the frequency range of 2.0~20 Hz. The excitation direction was east to west. The earthquakes were incrementally imposed, with starting motions with a weak acceleration level.

Accelerometers were attached to the east base stylobates and body stones of the two pagodas. A total of three different types of S3 pagoda models were assembled for the dynamic centrifuge tests. The lower and upper base stylobates of the first model were filled with weathered soil. The second model was assembled without them. In the third model, the contact area between stones was kept minimal. The roof stone and body stone were composed of a single stone each and the actual contact surface was closer to edge contact, as the surface was a slight concave. To reflect this, the surface was rubbed using sandpaper to establish four contacting sides. The acceleration history and frequency responses have been analysed for the three different pagoda models to compare their seismic behaviour.

A 1/15 model of the J5 pagoda was made and dynamic centrifuge tests on two types of J5 pagoda were performed. The base stylobates and the first body floor in the first model were filled with weathered soil and the second model was without them. The second and third floor of the J5 pagoda was turned slightly counter clock-wise, while the fourth and fifth floor were turned clock-wise. The roof stones were separate stone slabs and the length hanging outward was longer than the part weighed down by the upper body stone. There are signs of past conservation work to protect the roof stones from possible displacement and falling. There was a relatively large gap between the east side of the first roof stone and the base stylobate. Since the stone pagoda was composed of over 130 pieces of stone, the pagoda may have had structural issues caused by separation of the stones, displacement of blocks and fewer contact points. The most problematic structural instability of the pagoda seems to be the asymmetry of the fourth floor roof stone. The middle stone slab comprising the northern side of the fourth floor roof stone is twisted to the east. When observed from the west, the left side of the fourth floor roof stone is tilted northward. The model was built following the drawing of the original as closely as possible. In the processing of the model building, the factors that cause structural instability could be confirmed.

4.5 Test results in time domain

As shown in Figures 10 and 11, acceleration values were measured at different levels on the pagodas. The measurements were converted to the behaviour of the original pagoda in accordance with the scaling laws. Afterwards, amplification of peak acceleration was estimated and the seismic behaviour was compared for the three S3 and two J5 pagoda models. The results were calculated to the order of Ofunato and Hachinohe earthquake records. Figures 12 and 13 illustrate the amplification ratio of acceleration at different heights normalised by the peak ground surface acceleration.

No breakaway or fall of stone materials was observed in any of the three types of S3 and two types of J5 pagoda models even when the peak acceleration of ground surface was raised to 0.4 g and above during dynamic centrifuge tests. Given that the maximum design seismic acceleration specified in the Korean seismic design guide is 0.22 g and the amplification ratio of acceleration in the surrounding area of the pagoda ranges from 1.45~1.74, it can be concluded that the S3 pagoda and J5 pagoda are safe from a 2400 return period level earthquake, and the seismic resistance of the pagodas is excellent.

For S3 models 1, 2 and 3, it was observed that acceleration tended to be continuously amplified at

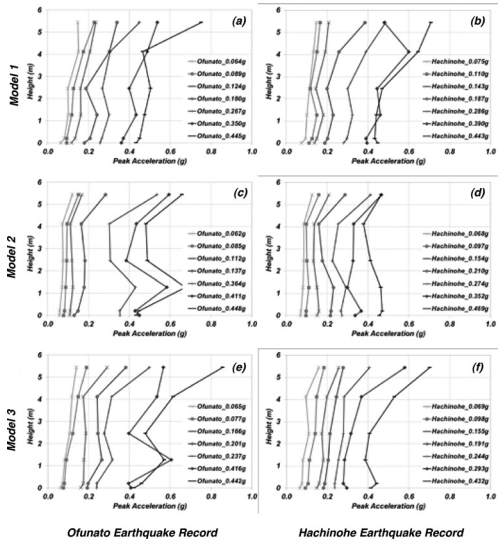


Figure 10. Variation of peak acceleration values for three types of S3 pagoda model (model 1: the base stylobates were filled with weathered soil, model 2: base stylobates without filler weathered soil, and model 3: the contact area between stones was kept minimal).

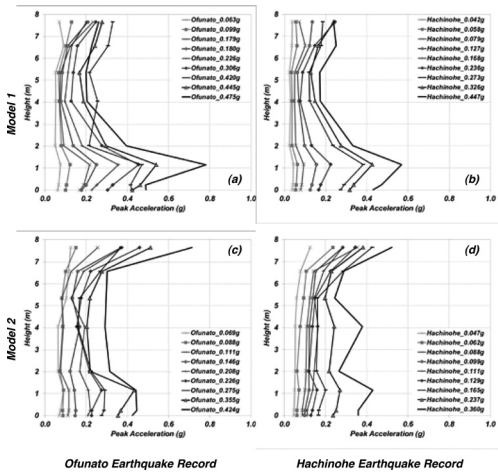


Figure 11. Variation of peak acceleration values for two types of J5 pagoda model (model 1: the base stylobates and the first body were filled with weathered soil and model 2: without filler weathered soil).

higher points. The body of the third floor showed at most 2.5 times amplification of acceleration in comparison to the ground surface. When the amplification ratio of acceleration was compared to the height of the three models, there was no significant difference: The amplification for the second floor

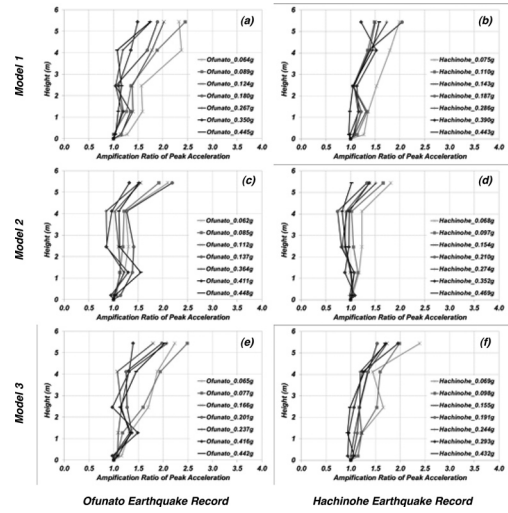


Figure 12. Normalised peak acceleration for peak ground surface acceleration with height for three types of S3 pagoda model.

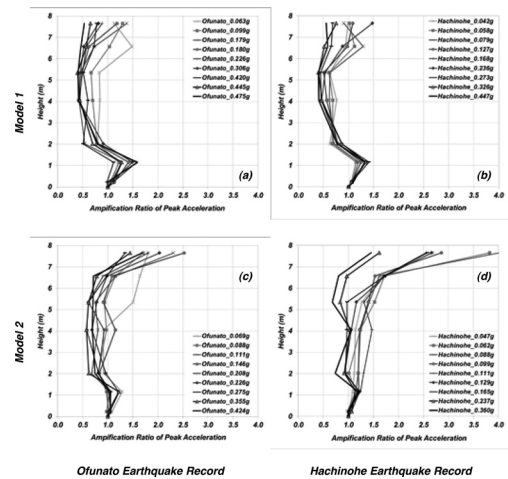


Figure 13. Normalised peak acceleration for peak ground surface acceleration with height for two types of J5 pagoda model.

body was greatest in model 3 followed by models 1 and 2. The average amplification from the base stylobate to the third floor body was within 15 percent variation.

Overall, the pagoda showed excellent seismic performance. Given the historical record of near-collapse due to an earthquake, a possible displacement or falling of the stones from the top part can be anticipated, but the pagoda proved stable against dynamic horizontal loading. Given that the body

stones and roof stones of the three stories all comprise a single stone each, the pagoda has a near symmetrical structure and the centre of gravity is steadily placed in the body of the first floor, it seems unlikely that a structural defect is the direct cause of the historic earthquake damage. It can be assumed from the test that the cause of the historical seismic damage was not dynamic instability of the structure. The cause is more likely to have been weakening stability of the pagoda structure due to differential settlement or the deformation of the southern ground from the collapse of the staircase and accessory facilities, or lowered stability of the base stylobate carapace stone caused by repetitive or dynamic normal stress and loss of fillers.

For J5 pagoda models 1 and 2, it was observed that acceleration tended to be amplified differently to that seen in the S3 pagoda. Figures 11 and 13 show that although the seismic waves imposed on the ground surface caused a maximum of 1.6 times amplification of the peak acceleration at the base stylobate, the seismic wave energy significantly reduced as it passed the first floor body, which was the longest stone in height. This tendency was shown especially in the test on model 1. In the first floor body (2.02 meters in height), the peak acceleration was reduced by 40 percent on average in comparison to the ground surface, and then the peak acceleration was gradually amplified again upwards. The greatest acceleration occurred in the upper part of the base stylobate and the fifth floor body, which was 1.6–1.9 times amplified compared to the ground surface. However, the amplification was very small. Overall, the pagoda body above first floor showed dispersion and reduction of the seismic load, rather than transfer and amplification. The J5 pagoda, comprising over 130 stones, demonstrates excellent seismic performance against dynamic lateral loading such as an earthquake.

4.6 Test results in frequency domain

By converting each of the measured acceleration values into the frequency domain, the pagodas' frequency response and natural frequency have been estimated. Using a sweeping signal (Fig. 1(c)), it can be confirmed whether the pagoda demonstrates amplification for a specific frequency at different heights. Figures 14 and 15 show the representative time history and frequency response of each seismic wave form for models 1, 2 and 3 of the S3 pagoda and models 1 and 2 of the J5 pagoda, respectively. The test results were scaled to those for the original pagoda prototypes according to the scaling laws for the frequency.

As shown in Figure 14, the frequency contents around 3.83 Hz was where the amplification

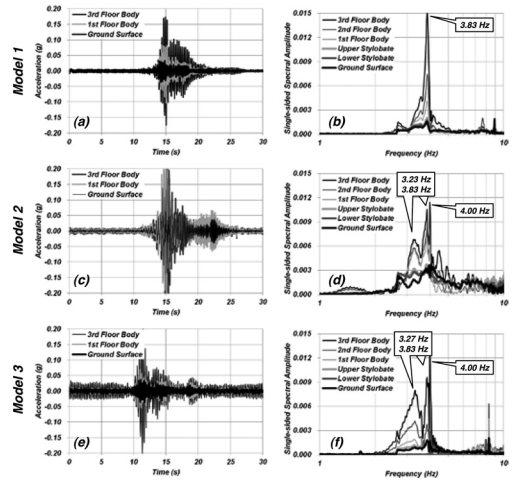


Figure 14. Time domain signal and its frequency response for the S3 pagoda during excitation of sweeping signal.

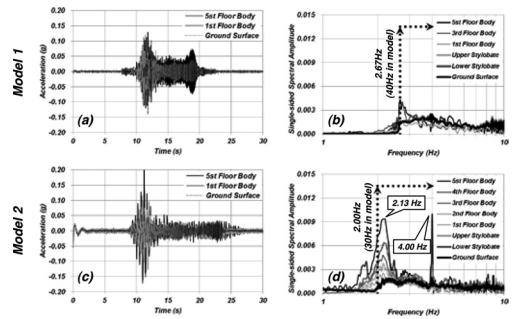


Figure 15. Time domain signal and its frequency response for the J5 pagoda during excitation of sweeping signal.

happened most clearly for the three models of the S3 pagoda. Models 2 and 3 showed amplification with height at 3.25 Hz. The amplification of 4.0 Hz, which is 60 Hz in a model at 15 g, can be considered to be the as electrical noise of an alternating current. The weight of fillers and the reduced contact area between stones did not have a significant impact on the natural frequency, 3.83 Hz, of the pagoda but resulted in the occurrence of another amplification frequency at 3.25 Hz.

It was observed that the repetition of the frequency of response in the test was maintained. The natural frequency of the pagoda is estimated as 3.83 and 3.25 Hz, depending on the status of filler and the current status of the contacting surface. In particular, amplification was observed repetitively and clearly at 3.83 Hz. It can be concluded that this

equates to the natural frequency in the case of lateral seismic wave excitation. According to seismic response analysis of the surrounding area, the natural period of the ground ranges from 0.13–0.15 seconds, which means the natural frequency ranges from 6.7–7.7 Hz. This means double amplification at the ground and pagoda structure is unlikely to happen in the event of seismic activity.

As aforementioned, the usable frequency range for the model is 30–300 Hz. For the dynamic centrifuge tests of the J5 pagoda, the excitation frequency ranges were different in model 1 and model 2. In the test for model 1, the sweeping signals, which had the frequency range of 40–300 Hz (2.67–20.0 Hz in prototype), were used. For model 2, frequency contents of 30–300 Hz (2.00–20.0 Hz in prototype) were used.

During the test, sweeping signals were imposed at 6 different levels for model 1 and 2. The frequency domain signals of model 1 did not reveal any consistent repetition or traits during dynamic signal excitation. The results failed to align partial seismic behaviour of each stone and the overall seismic behaviour of the pagoda. Due to the reduction of seismic wave energy in the first floor body, it seems that amplification at a specific frequency bandwidth is not likely to occur as shown in the upper sections of Figure 15.

However, the test results for model 2 of the J5 pagoda showed the amplification with heights at 2.13 Hz as shown in the lowers of Figure 15. This frequency is near to the boundary of excitation frequency at 2.0 Hz. However, it was considered that the repetition of the frequency response in the test was maintained in this study. It appears additional research is required to estimate the natural frequency of the J5 pagoda.

Given the large number of stones and structural instability, it can be assumed from the appearance that the J5 pagoda would not give a great seismic performance. When the findings from the S3 pagoda were compared with those of the J5 pagoda, the first floor body of the J5 pagoda showed energy dissipation and demonstrated complicated behaviour due to the relatively large number of stones. The test found that due to the reduction of seismic waves between the stylobate and the first floor body, the amplitude was not great in the event of an earthquake. The pagodas did not collapse at the peak acceleration defined in the Korean seismic design guide (Park et al., 2013a).

5 CONCLUSIONS

Modelling of models was conducted for three storey stone blocks. It was found that similar behaviour appears within a certain scope of error when

the results of the dynamic centrifuge tests for three models are reverted to the prototype scale. The results for modelling of models have ascertained that scaling laws act properly in three storey masonry structures when a horizontal seismic load acted on the structure. It showed the possibility of predicting the seismic behaviour of an actual structure if a model of the actual architectural heritage is produced and the seismic behaviour is assessed in conformity with the given scaling law. Therefore, it can be concluded that the seismic risk of the stone masonry structure can be assessed through dynamic centrifuge tests.

Models of two representative stone pagodas were produced and dynamic centrifuge tests were conducted. For the S3 pagoda models, it was observed that acceleration tended to be amplified with height. The third floor body showed at most a 2.5 times amplification of acceleration in comparison to the ground surface. This amplification was observed repetitively and clearly at a frequency of 3.83 Hz. For the J5 pagoda, the seismic wave energy significantly reduced as it passed the first floor body, and then the peak acceleration was gradually amplified again upwards. The two pagodas did not collapse at the peak acceleration defined in the Korean seismic design guide. It is no coincidence that the pagodas have stood under the skies of Gyeongju and Buyeo for 1300 years.

ACKNOWLEDGEMENTS

This research was supported by a Basic Science Research Program through the National Research Foundation of Korea (NRF) funded by the Ministry of Education, Science and Technology (grant number: 2009-0080575).

This study, which forms a part of the project, has been achieved with the support of national R&D project, which has been hosted by National Research Institute of Cultural Heritage of Cultural Heritage Administration. We express our gratitude to it.

The authors would like to thank Dr. Sei-Hyun Lee, Mr. Jeong-Gon Ha, Mr. Seong-Bae Jo, Mr. Hyung-Ik Cho and Ms. Sehee Kim for their advice and support in dynamic centrifuge testing.

REFERENCES

- Barkan, D.D. 1962. *Dynamic Bases and Foundations*, McGraw-Hill Book Company, New York.
- Borowicka, H. 1943. Uber ausmittig belastete, starre Platten auf elastisch-isotropem Untergrund, *Ingenieur-Archiv*, 14: 1–8.
- Buyeo-gun. 2005. *Safety Inspection of the Five storied stone pagoda of Jeongnimsa Temple site*, in Korean.

- Buyeo-gun, NRICH (National Research Institute of Cultural Heritage). 2009. *Data survey for historical research and restoration of Jeongnimsa Temple site, Buyeo*, in Korean.
- Bycroft, G.N. 1956. Forced vibrations of a rigid circular plate on a semi-infinite elastic space and on an elastic stratum, *Philosophical Transactions of the Royal Society A*, 248: 327–368.
- Das, B.M. & Ramana, G.V. 2010. *Principles of Soil Dynamics*, Second Edition, Cengage Learning.
- D'Ayala, D. & Ansal, A. 2012. Non-linear push over assessment of heritage buildings in Istanbul to define seismic risk, *Bulletin of Earthquake Engineering*, 10(1): 285–306.
- D'Ayala, D., Shi, Y. & Stammers, C. 2008. Dynamic multi-body behaviour of historic masonry buildings models, Structural Analysis of Historic Construction: Preserving Safety and Significance, *Two Volume Set: Proceedings of the VI International Conference on Structural Analysis of Historic Construction, SAHC08*, 2–4 July, Bath, United Kingdom, 489–496.
- Gorbunov-Possadov, M.I. & Serebrajanyi, R.V. 1961. Design of structures upon elastic foundations, *Proceedings, 5th International Conference on Soil Mechanics and Foundation Engineering*, 1, 643–648.
- Housner G. 1963. The behavior of inverted pendulum structures during earthquakes, *Bulletin of the Seismological Society of America* 53(2): 403–417.
- Ishiyama Y. 1982. Motions of rigid bodies and criteria for overturning by earthquake excitations, *Earthquake Engineering and Structural Dynamics* 10(5): 635–650.
- Itasca Consulting Group. 2001. FLAC 2D. Fast Lagrangian Analysis of Continua in 2 Dimensions, Version 4.0, User Manual, Minnea Police: Itasca.
- Kim, Dong-Soo, Kim, Nam-Ryong, Choo, Yun-Wook & Cho Gye-Chun. 2013a. A newly developed state-of-the-art geotechnical centrifuge in Korea. *KSCCE Journal of Civil Engineering*, 17(1): 77–84.
- Kim Dong-Soo, Lee, Sei-Hyun, Choo, Yun-Wook & Perdriat, Jacques. 2013b. Self-balanced earthquake simulator on centrifuge and dynamic performance verification. *KSCCE Journal of Civil Engineering*, 17(4): 651–661.
- Kim, Jae Kwan & Ryu, Hyeuk. 2003. Seismic test of a full-scale model of a five-storey stone pagoda. *Earthquake Engineering and Structural Dynamics* 32(5): 731–750.
- Kim, Yeong Taek, Lee Chan Hee & Lee, Myeong Seong. 2005. Deterioration assessment for conservation sciences of the five storied stone pagoda in the Jeongrimsaji Temple site, Buyeo, Korea. *Journal of the Korean Society of Economic and Environmental Geology* 38(6): 675–687, in Korean.
- Konstantinidis, Dimitrios & Makris, Nicos. 2005. Seismic response analysis of multidrum classical columns. *Earthquake Engineering and Structural Dynamics* 34(10): 1243–1270.
- Lee Chan Hee, Kim, Yeong Taek & Lee, Myeong Seong. 2007. Provenance presumption for rock properties of the five storied stone pagoda in the Jeongrimsaji Temple Site, Buyeo, Korea. *Journal of the geological society of Korea* 43(2): 183–196, in Korean.
- Makris, Nicos. & Konstantinidis, Dimitrios. 2003. The rocking spectrum and the limitations of practical design methodologies. *Earthquake Engineering and Structural Dynamics* 32(2): 265–289.
- NRICH (National Research Institute of Cultural Heritage). 2007. *Stone Stupa of Gyeongsangbuk-do I*, in Korean.
- Park, Heon-Joon, Kim, Derk-Moon, Kim, Ki-Seog, Ahn, Hee-Yoon & Kim, Dong-Soo. 2012. Noninvasive geotechnical site investigation for stability of Cheomseongdae. *Journal of Cultural Heritage* 13(1): 98–102.
- Park, Heon-Joon & Kim, Dong-Soo. 2013. Centrifuge Modelling for Evaluation of Seismic Behaviour of Stone Masonry Structure. *Soil Dynamics and Earthquake Engineering* 53: 187–195.
- Park, Heon-Joon, Kim, Dong-Soo & Choo, Yun-Wook. 2013a. Evaluation of the seismic response of stone pagodas using centrifuge model tests. *Bulletin of Earthquake Engineering*, Submitted.
- Park, Heon-Joon, Kim, Dong-Soo & Kim, Derk-Moon. 2013b. Seismic risk assessment of architectural heritages in Gyeongju considering local site effects. *Natural Hazards and Earth System Sciences* 13(2): 251–262.
- Peña, Fernando, Lourenço, Paulo B. & Campos-Costa, Alfredo. 2008. Experimental dynamic behavior of free-standing multi-block structures under seismic loadings. *Journal of Earthquake Engineering* 12(6): 953–979.
- Psycharis I. 1990. Dynamic behaviour of rocking two-block assemblies. *Earthquake Engineering and Structural Dynamics* 19(4): 555–575.
- Psycharis, I.N., Lemos, J.V., Papastamatiou, D.Y., Zambas, C. & Papantonopoulos, C. 2003. Numerical study of the seismic behaviour of a part of the Parthenon Pronaos. *Earthquake Engineering and Structural Dynamics* 32(13): 2063–2084.
- Schnabel, P.B., Lysmer, J. & Seed, H.B. 1972. SHAKE: a computer program for earthquake response analysis of horizontally layered sites. Report EERC 72-12, Earthquake Engineering Research Center, University of California, Berkeley.
- Spanos, P.D. & Koh, A.S. 1984. Rocking of rigid blocks due to harmonic shaking. *Journal of Engineering Mechanics* 110: 1627–1642.
- Spanos, Pol D., Roussis, Panayiotis C. & Politis, Nikolaos, P.A. 2001. Dynamic analysis of stacked rigid blocks. *Soil Dynamics and Earthquake Engineering* 21(7): 559–578.
- Stokoe, K.H., Hwang, S.K., Roesset, J.M. & SUN, W.S. 1994. Laboratory measurements of small-strain material damping of soil using the free-free resonant column, *Proceedings Earthquake Resistant Construction and Design*, Berlin, Germany, Balkema, Rotterdam, 195–202.
- Taylor, R.N. 1995. *Geotechnical centrifuge technology*, Blackie Academic and Professional, London.
- Tso, W. & Wong, C. 1989. Steady state rocking response of rigid blocks. Part 1: analysis. *Earthquake Engineering and Structural Dynamics* 18: 89–106.